ANS Reprint

ANALYSIS OF PLASMA BEHAVIOR IN A MAGNETIC THRUST CHAMBER OF A LASER FUSION ROCKET

INNOVATIVE CONCEPTS

KEYWORDS: *laser fusion rocket, Rayleigh-Taylor instability, thrust efficiency*

YOSHIHIKO NAGAMINE and HIDEKI NAKASHIMA*
Kyushu University, Department of Advanced Energy Engineering Science
6-1 Kasuga-Kouen Kasuga, Fukuoka 816, Japan

Received March 23, 1998
Accepted for Publication May 18, 1998

A magnetic thrust chamber concept in a laser fusion rocket is suitable for controlling the plasma flow, and it has an advantage in that thermalization with wall structures in a thrust chamber can be avoided. Rayleigh-Taylor instability would occur at the surface of expanding plasma, and it would lead to the degradation of thrust efficiency, which would result from diffusion of the plasma through an ambient magnetic field. A three-dimensional hybrid particle-in-cell code has been developed to analyze the plasma instability in the magnetic thrust chamber and to estimate the thrust efficiency. It is found that the instability would not have serious effects on the thrust efficiency; thrust efficiency in terms of momentum obtained here amounts to 65%. The effects of varying parameters on the thrust efficiency are also studied. The thrust efficiency seemed to reach its maximum value around $\theta_c = 50$ deg, where θ_c is an angle subtended from the initial plasma position at the z axis to the solenoidal coil and its dependence on magnetic field energy produced by the coil is found to be weak for the cases studied here.

I. INTRODUCTION

Fusion reaction can release a large amount of energy, and it could easily produce high-temperature and density plasma. The resulting plasma flow could be controlled by a properly designed applied magnetic field geometry, i.e., a magnetic thrust chamber. In a laser fusion rocket, the chamber is composed of a solenoidal superconducting coil. The fusion reaction occurs by irradiation of a laser onto a fuel pellet, and the plasma generated expands isotropically at an early stage; it is then deflected by the magnetic field and finally exhausted from the chamber. The chamber has an advantage in that thermalization with wall structures in a thrust chamber can be avoided. Thus, the laser fusion rocket could realize a very high exhaust velocity of plasma as compared with existing systems. This fact makes the laser fusion rocket a promising candidate for an interplanetary transport system.

Conceptual design studies of the laser fusion rocket have been performed.[1,2] For example, Hyde[1] designed a laser fusion rocket and estimated a thrust efficiency of the laser fusion rocket by using a two-dimensional magnetohydrodynamics (MHD) code. The efficiency in terms of momentum was reported to be 65%. Two-dimensional calculations have also been performed by Iinoya[3], but only for an early stage of the plasma flow in the chamber. The results from the experiments,[4–10] theoretical works, and computer simulations[11–18] for the expansion of plasma against an ambient magnetic field could give a perspective of the plasma behavior in the magnetic thrust chamber.

When both ion and electron are magnetized, the plasma expanding into the magnetic field can undergo Rayleigh-Taylor instability as the heavy fluid (plasma) is decelerated by the light fluid (magnetic field). For small amplitudes, the modes grow exponentially in time. From conventional MHD theory, the growth rate γ is given by

$$\gamma = \begin{cases} (g/L_n)^{(1/2)} & \text{for } kL_n \gg 1 \\ (kg)^{(1/2)} & \text{for } kL_n \ll 1 \end{cases} , \tag{1}$$

where

k = wave number

g = deceleration

L_n = scale length of the density gradient

$$= (\partial \ln n_i/\partial x)^{-1} , \tag{2}$$

n_i = ion density.

*E-mail: nakashima@aees.kyushu-u.ac.jp

The expanding plasma would exclude the ambient magnetic field, and a diamagnetic cavity would be formed.

On the other hand, when the ion is unmagnetized and the electron is magnetized (i.e., in the limit of a large-ion Larmor radius), the surface of the plasma develops the free streaming of the flute tips and bending of the flutes in the magnetic field as occurred in the Naval Research Laboratory laser experiments.[7] Hassam and Huba[18] proposed a new expression for γ in the limit of large Larmor radius (LLR) of the Rayleigh-Taylor instability:

$$\gamma = k(gL_n)^{(1/2)} \quad \text{for } kL_n \gg 1 \ . \tag{3}$$

They also calculated the development of the instability in the regimes of conventional and LLR Rayleigh-Taylor ones.[17] They showed that the strong diffusion across the magnetic field occurred in the regime of LLR Rayleigh-Taylor instability.

Zakharov et al.[6] found from their experiments that the magnetized parameter $L_B = \rho_i/R_b$ is an important one for understanding the behavior of the plasma expanding into a magnetic field, where $\rho_i = V_0/\omega_{ci}$ is a directed ion Larmor radius, V_0 is the initial plasma expansion velocity, and ω_{ci} is the cyclotron frequency. Then, R_b is the magnetic confinement radius at which the kinetic energy of the expanding plasma balances the excluded magnetic energy, which is defined as

$$R_b = \left(\frac{3\mu_0 E_p}{2B_0^2\pi}\right)^{1/3} , \tag{4}$$

where μ_0 is the vacuum permeability, E_p is the initial plasma kinetic energy, and B_0 is the initial magnetic field strength. In the case of $L_B > 1$, the expanding plasma behaves as the LLR Rayleigh-Taylor instability, while in the case of $L_B \ll 1$, it acts as the conventional one.

The numerical simulations have been performed to understand the behavior of a plasma expanding into the magnetic field by using MHD[17] and particle codes[12–16] in both two and three dimensions. Brecht and Thomas[11] calculated the expanding plasma against a magnetized background plasma by using two- and three-dimensional hybrid codes. Winske[15,16] calculated the linear and nonlinear behaviors of the Rayleigh-Taylor instability in a collisionless, magnetized plasma by using a two-dimensional hybrid code.

The instability may also occur at the boundary between the expanding plasma and the ambient decelerating magnetic field in the magnetic thrust chamber. The plasma would diffuse out through the magnetic field because of the instability, thereby leading to the degradation of the thrust efficiency. To examine the effects of the instability on the thrust efficiency in the magnetic thrust chamber, we developed a three-dimensional hybrid particle-in-cell (PIC) code.[20]

The purposes of this paper are to investigate (a) whether the Rayleigh-Taylor instability is significant for the plasma expanding in a laser fusion rocket's magnetic thrust chamber and (b) how the efficiency for converting particle momentum into momentum along the rocket's thrust vector varies with certain parameters.

The plan of the paper is as follows: Section II presents the calculational method and model adopted here. The analysis of plasma behavior in the magnetic thrust chamber and the estimation of a thrust conversion efficiency are presented in Sec. III along with discussion. The effects of varying parameters on the efficiency are also studied there. The conclusions are given in Sec. IV.

II. COMPUTATIONAL METHOD AND MODEL

The calculational model adopted here is illustrated in Fig. 1, which is based on a configuration of a laser fusion rocket proposed by Hyde.[1] The calculational parameters used in the simulation are shown in Table I. We proposed[21] to use ignition facilities such as the National Ignition Facility (NIF) to examine the feasibility of the magnetic thrust chamber concept because the facility could realize the same plasma conditions as supposed for the fusion rocket in terms of magnetization parameter L_B. Thus, the configuration studied here takes utilization of the facility into account; i.e., an NIF experimental configuration is treated here.

The fusion target, the indirect cryotarget, has a small deuterium-tritium fuel/CH ablator capsule inside a gold hohlraum, the target mass (113 mg) being dominated by gold. The target is irradiated by lasers with an energy of 1.8 MJ. A value of 20 MJ is adopted here for a representative fusion yield, 20% of which is carried by plasma. Its ionic charge is calculated from the simulation results for the NIF indirect drive target in Ref. 22 by using the Thomas-Fermi model.[23] A value of 16.81 is obtained for the ionic charge of gold at a temperature of 100 eV and a density of 1.0 g/cm^3. This charge number is given to all

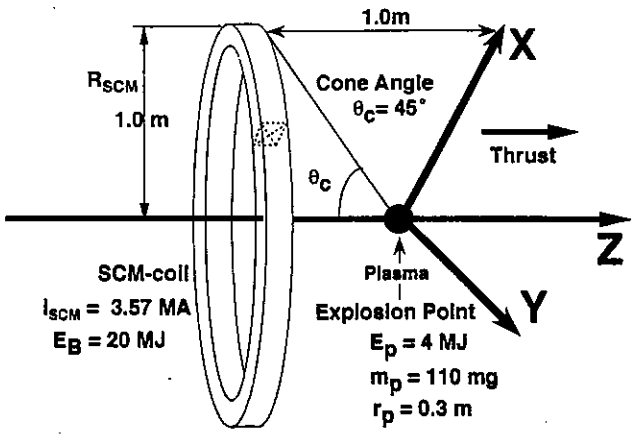

Fig. 1. Schematic of the calculational model.

TABLE I

Calculational Parameters

Plasma energy (MJ)	4
Plasma mass (mg)	110
Plasma radius (m)	0.3
Atomic mass (AMU)	197
Atomic number	79
Effective charge (C)	16.81
Electron temperature (eV)	0
SCM radius (m)	1.0
SCM current (MA)	3.57
Initial magnetic field strength at the coil axis (T)	2.12
Cone angle (deg)	45
Magnetized parameter L_B	1.82×10^{-2}
Cyclotron frequency ω_{ci} (s^{-1})	2.1×10^{7}
Expansion radius R_b (m)	0.71
Directed Larmor radius ρ_i (m)	1.29×10^{-2}
Initial plasma radius r_p (m)	0.3
Time step Δt (s)	4.8×10^{-9}
Calculational domain (m)	$6.0 \times 6.0 \times 7.0$
Mesh number	$60 \times 60 \times 70$
Number of particles simulated	100 000

the ions simulated. (The effect of the multiple ion species on the calculated behavior will be examined in future work.)

The initial plasma is assumed to have a radius r_p of 0.3 m and is entirely composed of gold, the mass m_p of which is 110 mg. The initial kinetic energy of plasma debris E_p is assumed as 4 MJ. The initial density and velocity distributions are assumed as uniform. The plasma is initialized with a 2% perturbation of mode $m = 50$ in the density.

The magnetic field in the chamber is generated by a solenoidal superconducting magnet (SCM) coil, which is, for convenience, approximated as a simple current loop with a radius R_{SCM} of 1.0 m and which carries a current I_{SCM} of 3.57 MA. The analytical solution for a vector potential produced by the loop is given in cylindrical coordinates as

$$A_\theta(r,\theta,z) = \frac{\mu_0 I_{SCM}\sqrt{R_{SCM}}}{\pi k\sqrt{r}} \times \left(\left(1-\frac{1}{2}k^2\right)K(k^2) - E(k^2)\right) , \quad (5)$$

where the argument of the elliptic integrals E and K is given by

$$k^2 = \frac{4rR_{SCM}}{(r+R_{SCM})^2 + (z-X)^2} , \quad (6)$$

where again X expresses the SCM coil position and r, θ, and z are taken as shown in Fig. 2. It is noted that A_θ is

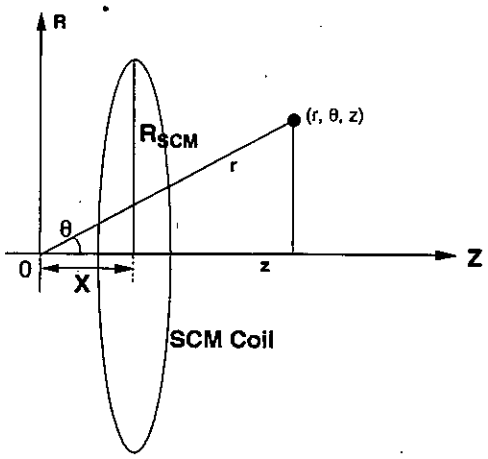

Fig. 2. Coordinate system for vector potential.

the only component that exists because the coil current is entirely in the θ direction. Then the magnetic flux $\boldsymbol{B}$ is obtained from the relation

$$\boldsymbol{B} = \nabla \times \boldsymbol{A} . \quad (7)$$

The initial magnetic field energy E_{Bi} is defined by

$$E_{Bi} = \tfrac{1}{2} L I_{SCM}^2 , \quad (8)$$

where L is the self-inductance of the coil, which is given by

$$L = \mu_0 R_{SCM}\left(\ln\frac{8R_{SCM}}{r_{SCM}} - \frac{7}{4}\right) , \quad (9)$$

where again r_{SCM} is a radius of the cross-sectional area of the coil and is set to be 0.21 m. The magnetic field energy E_B, which is obtained by summing over the computational region, is greater than the E_{Bi} because the magnetic field intensity near the coil is affected by the mesh size adopted and also by modeling of the coil. However, what really matters is the field that the plasma pushes against.[3] It is noted that the magnetic field intensity at the location of the plasma is not seriously changed by the adopted mesh size. Thus, E_B is used here for the ratio of the initial field energy to the initial plasma kinetic energy E_p. The coil produces a magnetic field intensity of 2.12 T at the center of the coil axis and stores about $E_B =$ 20 MJ ($E_{Bi} = 15$ MJ); i.e., the magnetic field energy E_B is five times greater than the initial plasma kinetic energy E_p. An angle θ_c (cone angle) subtended from the initial plasma position at the z axis to the solenoidal coil is taken to be 45 deg. Orth et al.[2] reported that the thrust efficiency reaches its maximum value around 50 deg.

The value of the magnetized parameter L_B is estimated as 1.82×10^{-2} for this study, the directed ion Larmor radius ρ_i being 1.29×10^{-2} m and the expanding radius R_b being 0.71 m, whereas a value of 4.96×10^{-4} is expected for the laser fusion rocket.[1] Thus, the value

of L_B here is much less than one as in the magnetic thrust chamber of the laser fusion rocket.

The dimensions ($X \times Y \times Z$) of the calculational region are $6 \times 6 \times 7$ m, and the calculational geometry is cylindrical along the z axis.

To calculate the plasma behavior in the magnetic thrust chamber, we developed a three-dimensional hybrid PIC code.[20] The basic equations in the code are as follows. Ampere's law is given by

$$\nabla \times \boldsymbol{B} = \mu_0(\boldsymbol{J}_e + \boldsymbol{J}_i) \ , \tag{10}$$

where $\boldsymbol{B}$ is the magnetic field vector, $\boldsymbol{J}_i$ and $\boldsymbol{J}_e$ are the ion and electron current densities, respectively, and μ_0 is the vacuum permeability, the transverse displacement current being neglected. We assume quasineutrality and set the ion density equal to the electron density; i.e., $n_i = n_e$. The kinetic equation of the electron fluid is given by

$$0 = -qn_e(\boldsymbol{E} + \boldsymbol{v}_e \times \boldsymbol{B}) - \nabla P_e \ , \tag{11}$$

where the inertia term and the resistivity are neglected. (The plasma cools as it expands, thereby causing some possible recombination. This phenomenon would lower the plasma conductivity and allow some of the magnetic field to possibly penetrate the plasma at its outer boundary. This would affect the growth of the Rayleigh-Taylor instability. We are trying to include the resistivity/conductivity into our code as formulated in Ref. 24. The results from the code will clarify the effect.) Here, $\boldsymbol{E}$ is the electric field vector, $\boldsymbol{v}_e$ the electron velocity, and P_e the electron pressure given by

$$P_e = n_e T_e \ , \tag{12}$$

where T_e is the electron temperature.

Eliminating $\boldsymbol{v}_e$ in Eq. (11) by using Eq. (10) and the definition of the electron current density

$$\boldsymbol{J}_e = -qn_e\boldsymbol{v}_e \ , \tag{13}$$

we obtain the following equation:

$$\boldsymbol{E} = \frac{1}{n_i}\left(\frac{1}{\mu_0 q}(\nabla \times \boldsymbol{B}) \times \boldsymbol{B} - \frac{1}{q}\boldsymbol{J}_i \times \boldsymbol{B} - \frac{T_e}{q}\nabla n_i\right) \ , \tag{14}$$

where Eq. (12) is used for P_e, assuming that the T_e is uniform. (The T_e is assumed to be zero in the simulation as given in Table I because the plasma cools down as it expands, and its internal energy will be converted into the kinetic energy.) The ion density n_i and the current density $\boldsymbol{J}_i$ are calculated by the PIC method from particle position $\boldsymbol{x}_i$ and velocity $\boldsymbol{v}_i$, which are obtained by solving the kinetic equations of an individual ion with mass M and charge q:

$$\frac{d\boldsymbol{v}_i}{dt} = \frac{q}{M}(\boldsymbol{E} + \boldsymbol{v}_i \times \boldsymbol{B}) \tag{15}$$

and

$$\frac{d\boldsymbol{x}_i}{dt} = \boldsymbol{v}_i \ . \tag{16}$$

The magnetic field is advanced by Faraday's law:

$$\frac{\partial \boldsymbol{B}}{\partial t} = -\nabla \times \boldsymbol{E} \ . \tag{17}$$

Cartesian coordinates are adopted here. The time advance of the field quantities is accomplished by a predictor-corrector algorithm, and the particle motion is followed by a leapfrog integrator.[20] The digital filter is used for the electric field.[25] The boundary condition adopted here for the field quantities is that the spatial differences of the normal components are set to be zero; i.e., a Neumann condition is adopted.

We checked the code against the dispersion relation of a magnetized plasma[20] and found good agreement between the analytical solutions and the numerical results.

III. RESULTS AND DISCUSSIONS

The plasma behaviors calculated by the three-dimensional hybrid PIC code are shown in Fig. 3, where we plot a series of the contours of plasma density in the x-y plane at $z = 0$ (Fig. 3a) and the x-z plane at $y = 0$ (Fig. 3b). The magnetic field vectors in the x-z plane are shown with arrows. The plasma initially expands isotropically, and then it is reflected back from the compressed magnetic field, resulting in thrust. The figure in the x-y plane shows that development of the instability is so weak that the instability would not seriously degrade the thrust efficiency.

A three-dimensional view of plasma density at 3 μs is shown in Fig. 4 for illustration. The plasma is pushed back by the magnetic field, and its shape is mushroomlike.

Figure 5 shows the magnetic field distributions at the initial time and 3.0 μs later in the magnetic thrust chamber. The magnetic field is excluded from the plasma region at 3.0 μs as compared with initial time: The diamagnetic cavity is formed as seen in the experiments of laser-produced plasmas expanding against an externally applied magnetic field.[19]

A series of plasma density distributions integrated over in the x-y plane along the z axis is shown in Fig. 6. The SCM coil is located at $z = -1.0$ m, its position being indicated as a gray line in Fig. 6. At an early stage, the density distribution is symmetrical about $z = 0$ where the initial plasma locates, then the plasma builds up between $z = 0$ m and $z = -1.0$ m, and the clump of plasma moves backward as the magnetic field pushes it back. The plasma that escaped toward the coil amounts to 5% at ~8 μs.

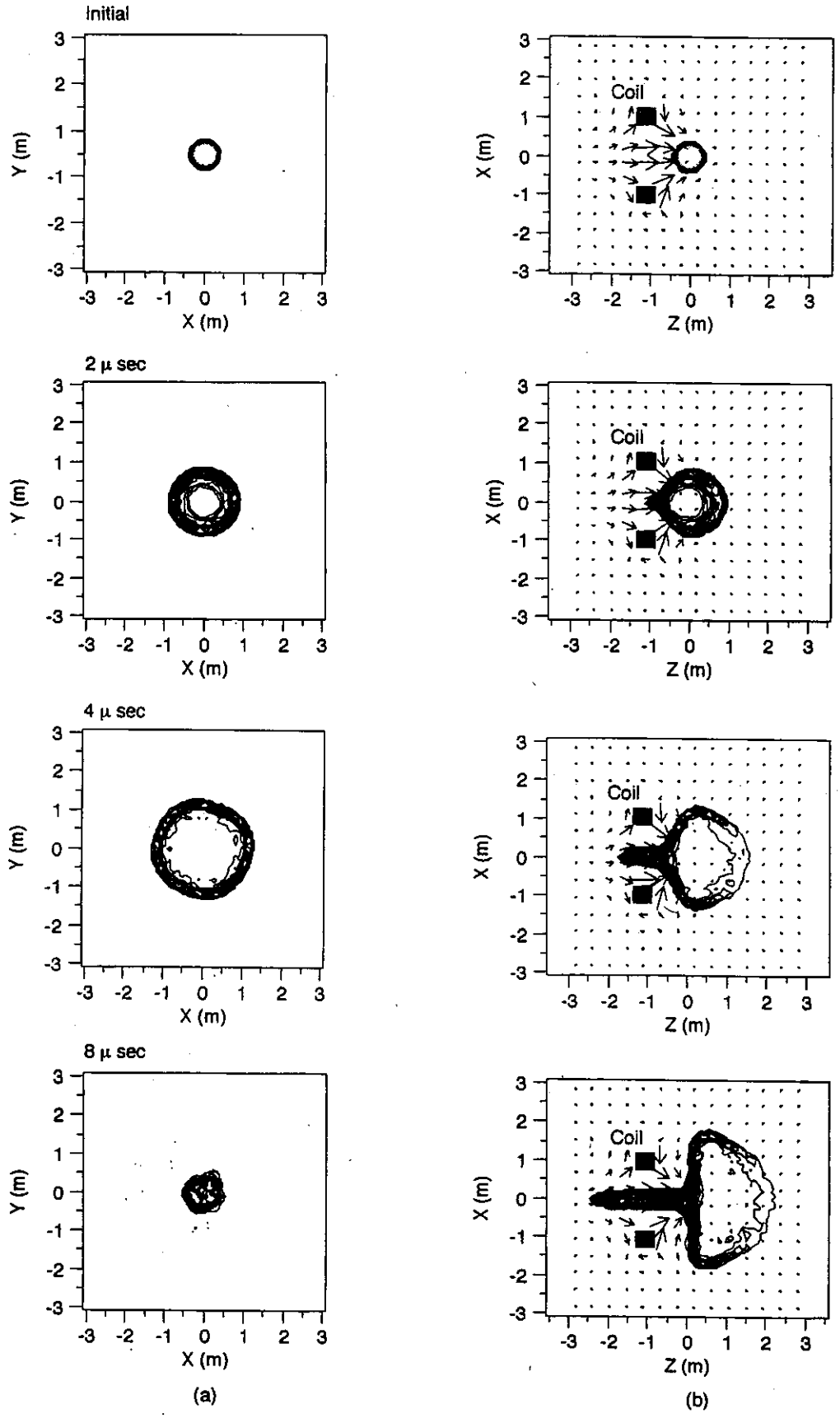

Fig. 3. Contour plots of plasma density: (a) plasma density in the x-y plane at $z = 0$; (b) plasma density in the x-z plane at $y = 0$.

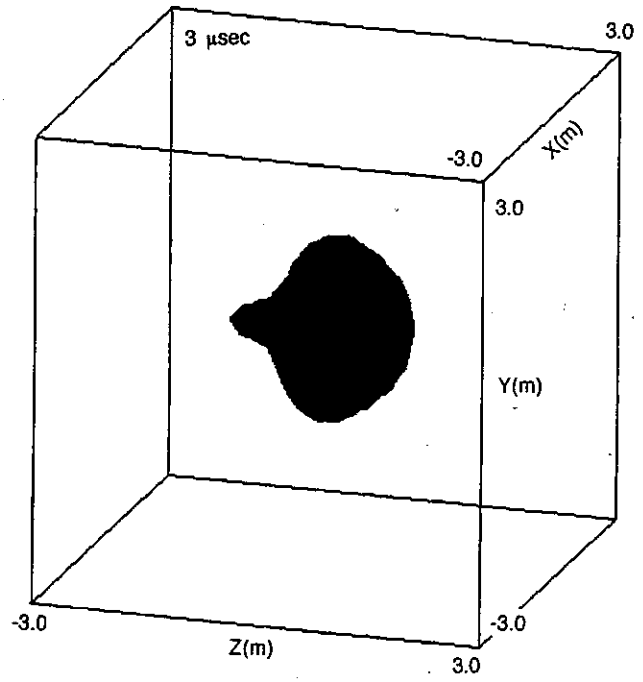

Fig. 4. Three-dimensional view of the plasma density at 3 μs.

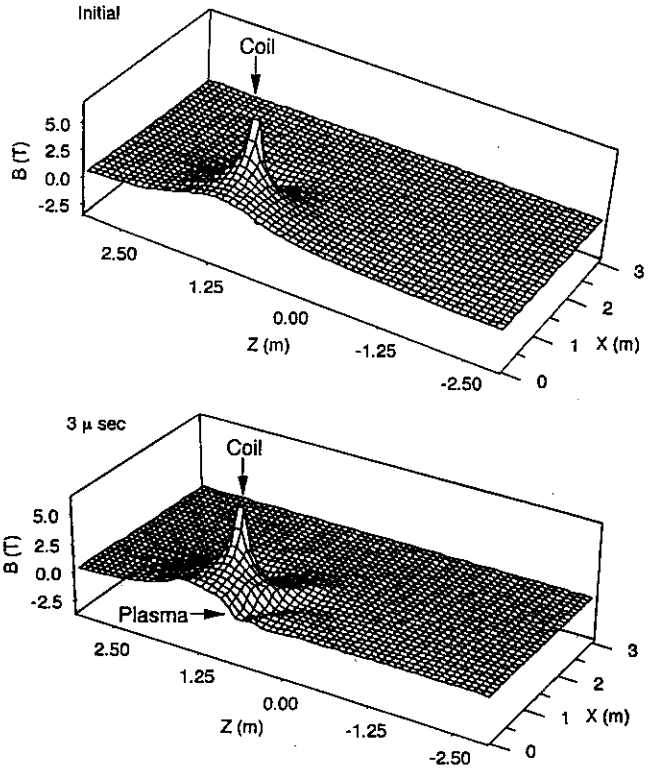

Fig. 5. Magnetic field distribution in x-z plane at $y = 0$.

The thrust efficiency η in terms of momentum is calculated as follows:

$$\eta = \frac{\sum M v_z}{\sum M |v_0|} , \qquad (18)$$

where M is the mass of ion, v_z the z-component of its velocity, and $|v_0|$ the absolute value of initial velocity. The sum (Σ) is carried over all plasma particles. The results are shown in Fig. 7 as a function of time. The value of η increases rapidly between 1 and 6 μs, and then its value saturates around 65% at ~8 μs. Figure 8 shows the time evolution of each component of the kinetic energy. It can be seen from the figure that the x and y components are converted into a z component with increasing time, which results in the increase of the thrust efficiency as shown in Fig. 7.

The instability on the plasma surface would develop well around $\phi = 45$ deg (toward the coil) as illustrated in Fig. 9 because the deceleration of the expanding plasma by the magnetic field is strongest in this direction. To analyze the growth rate of the instability in the magnetic thrust chamber, we stored an azimuthal-averaged plasma radius $\langle r \rangle$ between $\phi = 40$ and 50 deg and decomposed it into its azimuthal Fourier components m.

Figure 10 plots the time evolution of the amplitude for $m = 6$ as an example, and its amplitude grows exponentially after 3 μs. Around this time, the plasma ceases to expand and begins to turn around as shown in Fig. 11, where the averaged plasma position R as a function of time is represented as open circles. Thus, the growth rates are calculated after this time from the time evolution of the individual modes.

The instability in the magnetic thrust chamber is expected to be the conventional Rayleigh-Taylor instability because the magnetization parameter L_B is much less than one. The deceleration g can be determined from R in Fig. 11. These positions can be reasonably well represented by the parabola, $R = gt^2/2 + bt + c$ (the dashed line in Fig. 11) (Ref. 12). The inferred average deceleration $g = 1.13 \times 10^{11}$ m/s^2.

The density scale length L_n, the length over which the density drops by a factor of e, is obtained as $L_n = 0.1$ m from the simulation results.

Using the deceleration and scale length, we can estimate the instability growth rate from the expression given by Eq. (1). Figure 12 shows the theoretical growth rates (solid line) and the estimated rates from the simulation results (open circles) for modes $m = 2$ to 7. Modes $m = 5$ to 7 have growth rates that agree with the linear theory. (The growth rates of the Rayleigh-Taylor instability in the magnetized regime were also calculated in the case of ideal conditions by Winske,[15] and he reported there that the dominant modes are $m = 5$ and 6 and have growth rates that agree to the linear theory.) Modes $m = 2$ and 3 have growth rates that are greater than the linear theory because of the inherent noisiness

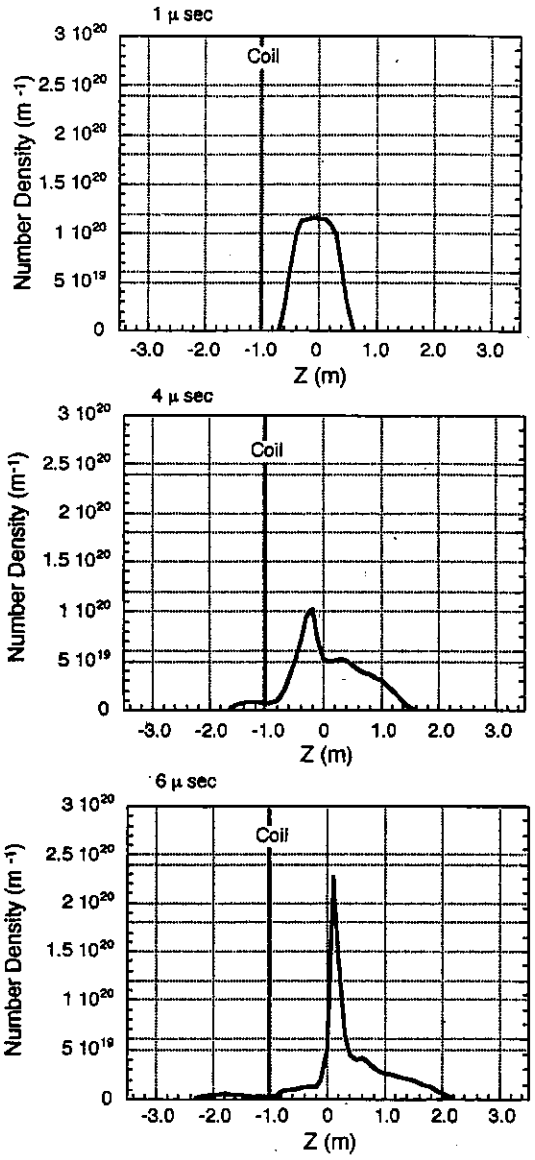

Fig. 6. Plasma mass distribution along z axis. The gray line indicates the coil position.

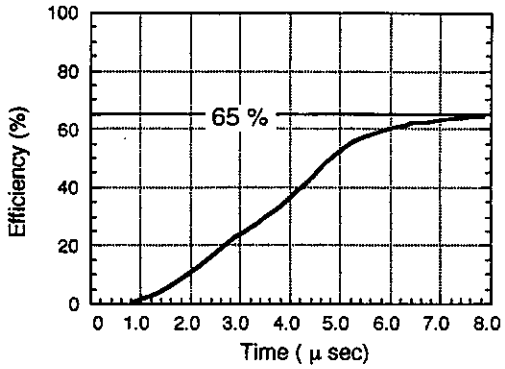

Fig. 7. Time evolution of the thrust efficiency for the case where $\theta_c = 45$ deg and E_B is five times greater than E_p.

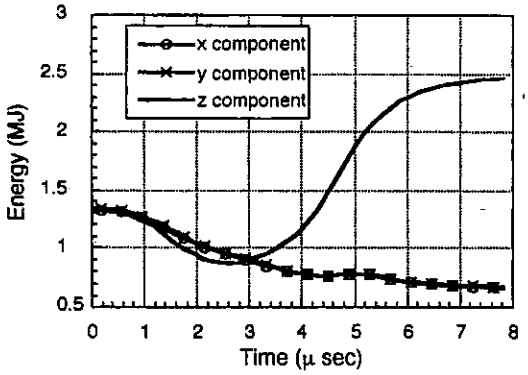

Fig. 8. Time evolution of each component of the plasma kinetic energy.

of the particle calculations.[15] However, the instability amplitude is so small, as shown in Figs. 3 and 4, that the instability would not have serious effects on the thrust efficiency. This is supported by the fact that the thrust efficiency calculated from the two-dimensional (r-z) PIC code also shows the same results obtained here.[26] The two-dimensional code is not capable of analyzing the instability treated here, and the results do not take account of the instability effect.

The parameters of the cone angle θ_c and magnetic field energy E_B produced by the solenoidal coil are varied to study their effects on the thrust efficiency η. Figure 13 shows the value of thrust efficiency as a function of θ_c, the open circles representing the simulation results and a solid line representing a fitted result by parabola. It indicates that there is a maximum value of η around 50 deg, which is consistent with the reported value in Ref. 2, and the sensitivity of the η to θ_c around 50 deg seems weak.

Figure 14 shows the η as a function of E_B, in which the open circles represent the simulation results. These calculations are performed under the condition of the fixed cone angle $\theta_c = 45$ deg because the $\theta_c = 45$ deg case will produce almost the maximum thrust efficiency η. The η value decreases as E_B decreases because the reflection of the plasma by the magnetic field becomes weaker; however, the value of η still remains 56% for the case of $E_B = 12$ MJ ($E_{Bi} = 11.8$ MJ); i.e., the value of E_B is three times greater than that of E_p. The results are desirable from the engineering viewpoint because the reduction in the required magnetic field energy means that in the required SCM coil current.

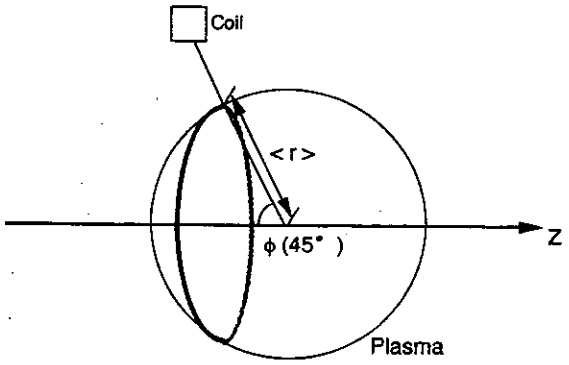

Fig. 9. Schematic of the sampling method and mode analysis for the averaged plasma radius.

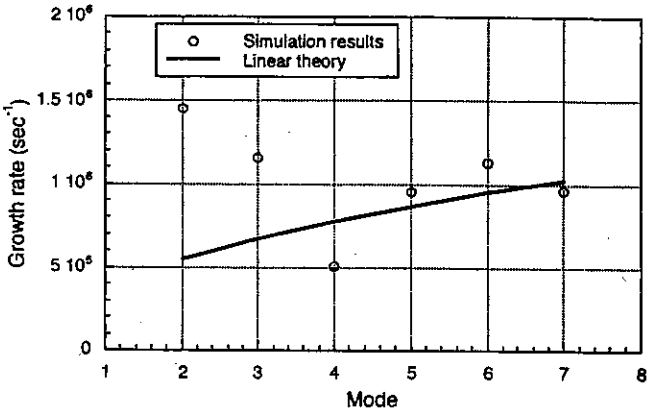

Fig. 12. The growth rates for modes $m = 2$ to 7.

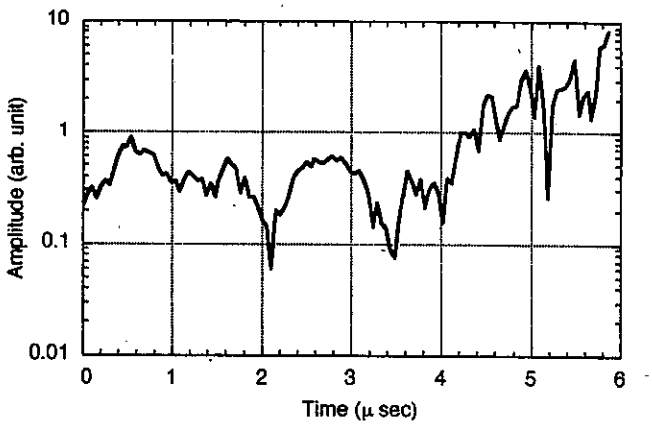

Fig. 10. Time evolution of the amplitude for $m = 6$.

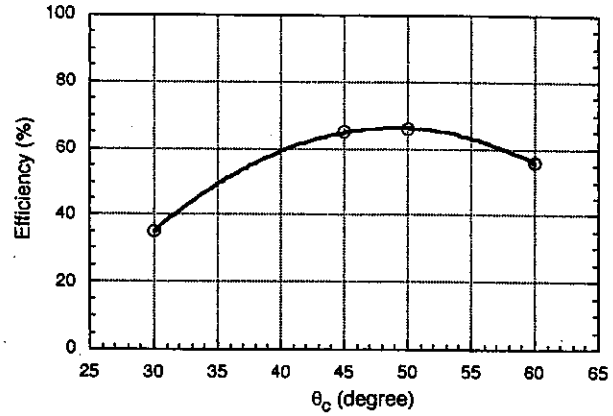

Fig. 13. Thrust efficiency as a function of θ_c.

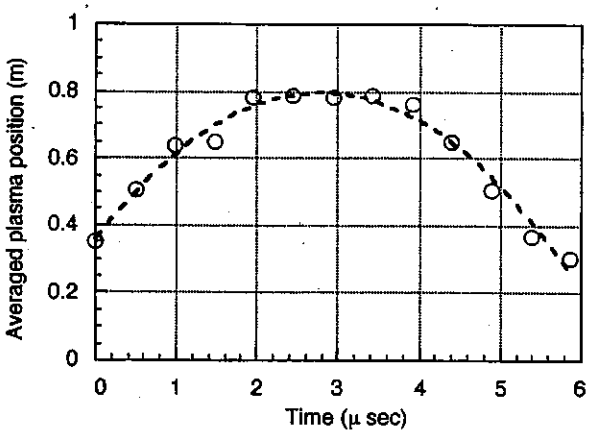

Fig. 11. Time evolution of the averaged plasma radius.

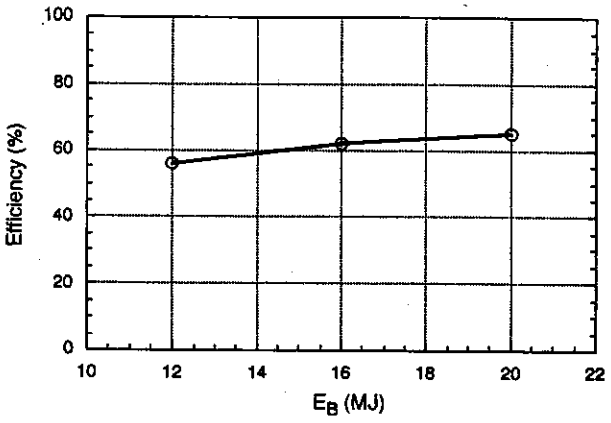

Fig. 14. Thrust efficiency as a function of E_B.

IV. CONCLUSION

To analyze the plasma behavior in the magnetic thrust chamber for a laser fusion rocket, the three-dimensional hybrid PIC code was developed. By using the code, we found that the thrust efficiency in terms of momentum is found to be 65% for the case where the cone angle θ_c = 45 deg and the magnetic field energy E_B is five times

greater than the initial plasma kinetic energy E_p. The fraction of the plasma density that escapes toward the coil is found to be 5%.

The growth rates for the instability are estimated. The growth rates of mode $m = 5$ to 7 are found to agree with the linear theory, and those of mode $m = 2$ and 3 are greater than the linear theory. However, the instability would not have serious effects on the thrust efficiency because the instability amplitude is very small. This is supported by the fact that the thrust efficiency calculated from the two-dimensional (r-z) PIC code shows the same results as obtained here.

The study of the effects on the thrust efficiency is performed when the cone angle θ_c and magnetic field energy E_B are varied. The thrust efficiency seemed to reach its maximum value around $\theta_c = 50$ deg for the case where E_B is five times greater than E_p. The thrust efficiency is still 56% for the case where E_B is three times greater than E_p.

Although there are numerical limitations (e.g., neglect of the plasma resistivity) that must be removed in future work, these results would give valuable information in designing the laser fusion rocket.

ACKNOWLEDGMENT

The computations were performed with the SX-4 at the National Institute for Fusion Science.

REFERENCES

1. R. A. HYDE, UCRL-88857, Lawrence Berkeley Laboratory (1983).

2. C. D. ORTH et al., AIAA-87-1904 (1987).

3. F. IINOYA, PhD Thesis, California Institute of Technology (1993).

4. S. OKADA et al., *Jpn. J. Appl. Phys.*, **20**, 157 (1981).

5. H. DICKINSON et al., *Phys. Fluids*, **5**, 1048 (1962).

6. YU. P. ZAKHAROV et al., *Sov. J. Plasma Phys.*, **12**, 674 (1986).

7. B. H. RIPIN et al., *Phys. Rev. Lett.*, **59**, 2299 (1987).

8. P. A. BERNHARDT et al., *J. Geophys. Res.*, **92**, 5777 (1987).

9. J. D. HUBA et al., *J. Geophys. Res.*, **97**, 11 (1992).

10. B. H. RIPIN et al., *Phys. Fluids*, **B5**, 3491 (1993).

11. S. H. BRECHT and V. A. THOMAS, *J. Geophys. Res.*, **92**, 2289 (1987).

12. A. G. SGRO et al., *Phys. Fluids*, **B1**, 1890 (1989).

13. D. WINSKE, *Phys. Fluids*, **B1**, 1900 (1989).

14. S. H. BRECHT and N. T. GLADD, *IEEE Trans. Plasma Sci.*, **20**, 678 (1992).

15. D. WINSKE, *Phys. Plasmas*, **3**, 3966 (1996).

16. D. WINSKE, *Phys. Plasmas*, **4**, 2454 (1997).

17. J. D. HUBA et al., *Phys. Rev. Lett.*, **59**, 2971 (1987).

18. A. B. HASSAM and J. D. HUBA, *Phys. Fluids*, **31**, 318 (1988).

19. YU. P. ZAKHAROV et al., *Proc. Int. Conf. Plasma Physics*, **2**, 1670 (1996).

20. J. E. HOROWITZ et al., *J. Comput. Phys.*, **84**, 279 (1989).

21. H. NAKASHIMA et al., to be published in *Fusion Engineering and Design* (1998).

22. R. P. PETERSON et al., UWFDM-1008, University of Wisconsin, Madison (1996); see also R. P. PETERSON et al., *Fusion Technol.*, **30**, 431 (1996).

23. R. M. MORE, UCRL-84991, Lawrence Berkeley Laboratory (1981).

24. K. R. MOORE et al., *J. Geophys. Res.*, **96**, 7779 (1991).

25. C. K. BIRDSALL and A. B. LANGDON, *Plasma Physics via Computer Simulation*, McGraw Hill, New York (1985).

26. N. YOSHIMI, Private Communication (1998).

Yoshihiko Nagamine (MS, Kyushu University, Japan, 1995) is a graduate student in the Department of Energy Conversion Engineering. His research interests include the plasma process, negative ion sources, and laser wake field acceleration.

Hideki Nakashima (D Eng, Kyushu University, Japan, 1978) is a professor in the Department of Advanced Energy Engineering Science at Kyushu University. His research interests include fusion energy conversion, fusion reactor engineering, and plasma propulsion.